

Effects of anisotropy, aspect ratio, and nonstraightness of carbon nanotubes on thermal conductivity of carbon nanotube composites

Fei Deng, Quan-Shui Zheng,^{a)} and Li-Feng Wang

Department of Engineering Mechanics, Tsinghua University, Beijing 100084, People's Republic of China

Ce-Wen Nan

Department of Materials Science and Engineering, Tsinghua University, Beijing 100084, People's Republic of China

(Received 27 September 2006; accepted 5 December 2006; published online 10 January 2007)

Simple models for the thermal conductivity enhancements in carbon nanotube (CNT) composites are presented as analytical functions of volume fraction, anisotropic thermal conductivities, aspect ratio, nonstraightness, and interfacial thermal resistance of the CNTs. The model predictions agree very well with the measured thermal conductivities of CNT composites available in the literature. It is shown that using CNTs with higher aspect and straightness ratios is an efficient means to get much better thermal conductivity enhancements for CNT composites. The models are further extended to account the effects of either the random or aligned orientation of CNTs and the interaction among CNTs on thermal conductivity of CNT composites. © 2007 American Institute of Physics. [DOI: 10.1063/1.2430914]

The supermechanical, thermal, and electrical properties of carbon nanotubes (CNTs) and their one-dimensional characteristic have led to ever increasing interests in studying CNT-based devices and composites.¹ For example, the axial thermal conductivity of CNTs was found to be extremely high, about 2000 W/mK (Ref. 2) or more than 3000 W/mK (Ref. 3) for multiwalled CNTs and even higher for single walled CNTs,^{4,5} and the thermal conductivities of CNT-in-oil suspensions and CNT-in-polymer composites were observed to be significantly improved^{6,7} up to, for example, a 150% increase at 1% volume fraction of CNTs.⁷ Several theoretical predictions on the thermal conductivity enhancements in CNT composites have been proposed in the literature. Compared with the experimentally observed data,⁷ the prediction by modeling the CNTs as spherical inclusions or infinitely long fibers, respectively, terribly underestimates⁷ or overestimates⁸ the thermal conductivity enhancements. An improved prediction⁹ was given by incorporating an interfacial thermal resistance.¹⁰⁻¹² A recent theoretical study¹³ further showed that the tube-end heat transport property is a more significant factor of affecting the effective thermal conductivity, rather than the thermal contact resistance on the lateral surfaces of the CNTs.

We note that the CNTs used in the experiments⁷ are multiwalled carbon nanotubes (MWNTs) with the diameters about 25 nm, have very large but finite aspect ratios (approximately 2000), and are not straight. We also note that the above-mentioned theoretical predictions are based on the isotropy assumption for the thermal conductivity of CNTs, while the thermal conductivity of graphite is known to be highly anisotropic. The measured thermal conductivities of graphite in the basal plane range from 940 to 2000 W/mK, and those normal to the basal plane are two or three orders lower (between 5 and 20 W/mK).¹⁴ For highly oriented pyrolytic graphite, the ratios of the basal thermal conductivity to the normal one can be even larger.¹⁵ Since MWNTs have

a curled graphite structure, it is expected that their axial and transverse thermal conductivities would be similar to those of the graphite basal and normal ones and thus be quite different, because of the very weak van der Waals interwall interaction. Indeed, there have been molecular simulations¹⁶ that predicted the axial and transverse thermal conductivities of CNT bundles to be very close to the basal and normal ones of graphite, although there have been no measurements of the radial thermal conductivity of CNTs. The above observations raise the need to systematically examine the effects of the thermal conductivity anisotropy, aspect ratio, and nonstraightness of CNTs on the effective thermal conductivities of CNT composites. With regard to the thermal anisotropy, we may need to further claim an exception that the radial thermal conductivity of individual single-walled carbon nanotubes may be much larger than those of MWNTs because the former have no wall-to-wall interaction. However, the CNTs used in the experiments⁷ are MWNTs.

In what follows we first give an analytical model of thermal conductivity for CNT composites with low loadings of randomly oriented CNTs. For estimating the mechanical and thermal properties of inclusion-in-matrix composites, even though for those with high concentrated inclusions so that interactions among inclusions must be considered, some mature methods have been established within the framework of the micromechanics.^{17,18} For CNT composites with low loadings of randomly oriented straight CNTs of average length L and diameter d , an analytical estimate for the effective thermal conductivities, k_e , of the CNT composites can be given in the following form:

$$\frac{k_e}{k_m} = 1 + \frac{f}{3} \left[\frac{1}{(k_{33}^c/k_m - 1)^{-1} + H} + \frac{2}{(k_{11}^c/k_m - 1)^{-1} + (1 - H)/2} \right], \quad (1)$$

where f denotes the volume fraction of the CNTs, k_{33}^c and k_{11}^c denote the axial and transverse thermal conductivities of the CNTs, k_m denotes the thermal conductivity of the isotropic

^{a)}Author to whom correspondence should be addressed; electronic mail: zhengqs@tsinghua.edu.cn

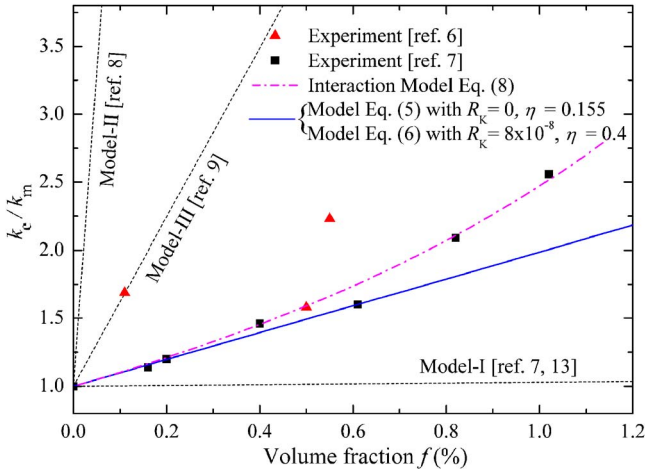


FIG. 1. (Color online) Measured and predicted thermal conductivity enhancements in the composites filled with low loadings of CNTs. The same parameters ($k_c=2000$ W/mK, $k_m=0.1448$ W/mK, and $p=2000$) are used for both the experiments and predictions.

matrix, and H reflects the influence of the aspect ratio, $p=L/d$, in the form

$$H(p) = \frac{1}{p^2-1} \left[\frac{p}{\sqrt{p^2-1}} \ln(p + \sqrt{p^2-1}) - 1 \right]. \quad (2)$$

It is important to note that the analytical expression Eq. (1) is precise up to the first order of f as $f \rightarrow 0$, and takes account of not only the effect of the thermal conductive anisotropy of the CNTs through the two dimensionless parameters k_{33}^c/k_m and k_{11}^c/k_m , but also the influence of the aspect ratio, p , of CNTs through the single dimensionless factor H in the ideal case that the CNTs would be all straight.

The function $H(p)$ monotonously decreases from $1/3$ to 0 as p changes from 1 (for regarding CNTs as spherical inclusions) to ∞ (for modeling CNTs as infinitely long fibers). We obtain the so-called model-I prediction^{7,13} $k_e/k_m=1+3f$ from Eq. (1) by assuming the thermal isotropy ($k_{11}^c=k_{33}^c=k_c$) with $k_c/k_m \gg 1$ and the spherical inclusions for CNTs ($p=1$ and $H=1/3$). As indicated in Fig. 1, the model-I predictions terribly underestimate the thermal conductivity enhancements. In fact, typical CNTs have aspect ratios in the order of 1000 or even larger. We note that the values of $k_m=0.1448$ W/mK and $k_{33}^c=2000$ W/mK estimated in the experiments⁷ lead to a very small quantity of $(k_{33}^c/k_m-1)^{-1}=7.24 \times 10^{-5}$. In comparison, the values of H ranging from 1.0×10^{-4} to 1.0×10^{-6} as increasing p from 230 to 2800 , as shown in Fig. 2(a), indicate that $(k_{33}^c/k_m-1)^{-1}$ and H can be similarly small. Therefore, the H in the denominator of the first term in the square bracket in Eq. (1) can have notably contribution while the whole second term in the square bracket is four orders smaller than the first term and thus is negligible. The above analyses yield the following excellent approximation of Eq. (1):

$$\frac{k_e}{k_m} = 1 + \frac{f/3}{k_m/k_{33}^c + H}. \quad (3)$$

Compared with Eq. (3), the following so-called model-II (Ref. 8) and model-III (Ref. 9) predictions:

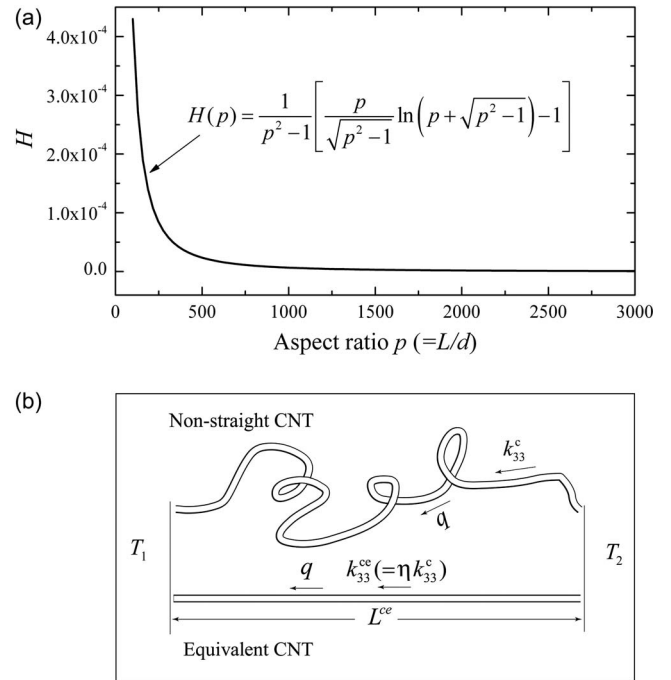


FIG. 2. (a) Dependence of $H(p)$ on the aspect ratio $p (=L/d)$. (b) A schematic illustration of the nonstraight and equivalent CNTs.

$$\frac{k_e}{k_m} = 1 + \frac{f}{3} \frac{k_c}{k_m}, \quad \frac{k_e}{k_m} = 1 + \frac{f}{3} \frac{k_{33}^{cs}}{k_m}, \quad (4)$$

respectively, ignored the influence of H , where $k_{33}^{cs}=k_c/(1+2R_K k_c/L)$ is the equivalent axial thermal conductivity of CNTs coated with interfacial thermal resistance layers of the Kaptiza resistance,¹⁰⁻¹² R_K .

Microscopic observations show that well-dispersed and low loaded CNTs in composites are often far from being straight due to their very large aspect ratios. For a nonstraight CNT as schematically illustrated in Fig. 2(b), the high thermal anisotropy ($k_{11}^c/k_{33}^c \ll 1$) of CNTs induces a unique property that individual CNTs are nearly perfect one-dimensional thermal cables with negligibly small thermal flux losses during long distance thermal conductions. For a nonstraight CNT with length L under a two-end temperature difference, $\Delta T=T_2-T_1$, as illustrated in Fig. 2(b), the thermal flux q is equal to $k_{33}^c \Delta T/L$ because of the thermal cable property of the CNT. On the other hand, we can regard this CNT as an equivalent straight thermal cable such that the same thermal flux q is conducted [Fig. 2(b)] between the two ends of the CNT in the distance L^{ce} . The above analyses yield the following refined model:

$$\frac{k_e}{k_m} = 1 + \frac{\eta f/3}{k_m/\eta k_{33}^c + H(\eta p)}, \quad (5)$$

with $k_{33}^{ce}=\eta k_{33}^c$ the thermal conductivity of the equivalent straight thermal cable and $\eta=L^{ce}/L$ the straightness ratio of the CNTs.

To analyze in more detail the effects of aspect ratio and nonstraightness, we plot in Fig. 1 the predicted values k_e/k_m by the refined model (5) versus the volume fractions f of the CNTs in comparison with the two sets of recent experimental data^{6,7} as well as the predictions by models I-III. In these predictions, the same values of $k_m=0.1448$ W/mK, $k_{33}^c=2000$ W/mK, and $\eta \approx 2000$ (corresponding to the average

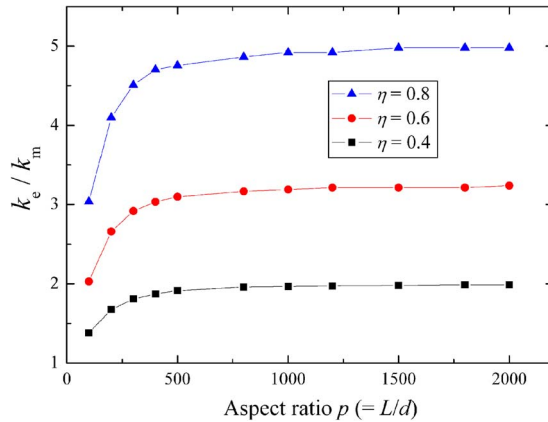


FIG. 3. (Color online) Effects of aspect ratio p and straightness ratio η on thermal conductivity enhancement predicted by the model Eq. (6) with $k_{33}^c=2000$ W/mK, $k_m=0.1448$ W/mK, and $R_K=8\times 10^{-8}$ m² K/W.

CNT length of 50 μm and diameter of 25 nm) as the measured ones in the experiments⁷ are adopted. The results shown in Fig. 1 indicate that the prediction from the present model Eq. (5) with $\eta=0.155$ can agree well with the measured thermal conductivity enhancements. The further results shown in Fig. 3 indicate that larger straightness ratios η and larger aspect ratios p lead to better thermal enhancement effects, and the enhancement effects tend to be saturated for larger p than 500.

We note that an interesting and important function of the lateral interfacial thermal resistance is to further reduce the transverse thermal conductivity to a lower level than the k_{11}^c and thus improve the thermal cable property of CNTs. The influence of the tube-end thermal resistance can be reflected by modifying the k_{33}^c in Eq. (5) with the effective one $k_{33}^{\text{cs}}=k_{33}^c/(1+2R_Kk_{33}^c/L)$, that is,

$$\frac{k_e}{k_m} = 1 + \frac{\eta f/3}{k_m/\eta k_{33}^{\text{cs}} + H(\eta p)}. \quad (6)$$

As shown in Fig. 1, the same excellent prediction can be achieved with $\eta=0.4$ and the Kaptiza resistance $R_K=8\times 10^{-8}$ m² K/W.

For CNT composites with aligned straight CNTs in one direction, x_3 axis, the corresponding analytical formulas for the axial and transverse thermal conductivity enhancements are

$$\begin{aligned} \frac{k_{33}}{k_m} &= 1 + \frac{f}{k_m/k_{33}^c + H}, \quad \frac{k_{11}}{k_m} = 1 \\ &+ \frac{f}{(k_{11}^c/k_m - 1)^{-1} + (1 - H)/2}. \end{aligned} \quad (7)$$

The enhancement, $k_{33}^e/k_m - 1$, with the aligned CNTs is three times of that with the randomly oriented CNTs while the transverse enhancement, $k_{11}^e/k_m - 1$, is four orders in magnitude smaller than $k_{33}^e/k_m - 1$. Similar extensions as those from Eq. (3) to Eqs. (5) and (6) for accounting the effects of nonstraightness and tube-end Kaptiza resistance can be given.

Finally, using the interaction direct derivative (IDD) micromechanics scheme¹⁸ we can give the following analytical estimate:

$$\frac{k^{\text{IDD}}}{k_m} = 1 + \left[1 - H(q) \left(\frac{k_e}{k_m} - 1 \right) \right]^{-1} \left(\frac{k_e}{k_m} - 1 \right) \quad (8)$$

to take account of the interaction effect among CNTs, where k_e/k_m is the noninteraction estimate given by either Eq. (3) and (5), or (6); and $H(q)$ is the function of q in the form Eq. (2), with^{18,19} $q=1$ corresponding to the random or isotropic distribution. The very good nonlinear enhancement prediction shown in Fig. 1 indicates that the interaction effect among CNTs can be notable even though for very low loadings of CNTs.

In conclusion, we present analytical but still simple formulas for predicting the thermal conductivities of CNT composites with low loadings of CNTs that take account of the effects of the thermal conductivity anisotropy, aspect ratio, nonstraightness, interfacial thermal resistance, interaction, and either random or aligned distribution of the CNTs. The excellent agreements between the measured data and the predicted ones using these formulas indicate that the finite aspect ratios and nonstraight geometries of the CNTs as well as the tube-end thermal resistance have the dominant influences to the effective thermal conductivity properties of CNT composites, rather than the lateral interfacial thermal resistance. The analyses show that using as straight as possible CNTs with aspect ratios not lower than 500 is a very efficient means to get much better thermal conductivity enhancements for CNT composites. It is further shown that the previously observed nonlinear behavior on the enhancements versus low loadings of CNTs is attributed to an interaction effect among CNTs.

¹R. H. Baughman, A. A. Zakhidov, and W. A. de Heer, *Science* **297**, 787 (2002).

²M. Fujii, X. Zhang, H. Xie, H. Ago, K. Takahashi, and T. Ikuta, *Phys. Rev. Lett.* **95**, 065502 (2005).

³P. Kim, L. Shi, A. Majumdar, and P. L. McEuen, *Phys. Rev. Lett.* **87**, 215502 (2001).

⁴E. Pop, D. Mann, Q. Wang, K. Goodson, and H. Dai, *Nano Lett.* **6**, 1 (2006).

⁵C. Yu, L. Shi, Z. Yao, D. Li, and A. Majumdar, *Nano Lett.* **5**, 1842 (2005).

⁶M. J. Biercuk, M. C. Llagunno, M. Radosavljevic, J. K. Hyum, A. T. Johnson, and J. E. Fischer, *Appl. Phys. Lett.* **80**, 2767 (2002).

⁷S. U. S. Choi, Z. G. Zhang, W. Yu, F. E. Lockwood, and E. A. Grulke, *Appl. Phys. Lett.* **79**, 2252 (2001).

⁸C. W. Nan, Z. Shi, and Y. Lin, *Chem. Phys. Lett.* **375**, 666 (2003).

⁹C. W. Nan, G. Liu, Y. Lin, and M. Li, *Appl. Phys. Lett.* **85**, 3549 (2004).

¹⁰S. Huxtable, D. G. Cahill, S. Shenogin, L. Xue, R. Ozisik, P. Barone, M. Usrey, M. S. Strano, G. Siddons, M. Shim, and P. Kebinski, *Nat. Mater.* **2**, 731 (2003).

¹¹C. W. Nan, R. Birringer, D. R. Clarke, and H. Gleiter, *J. Appl. Phys.* **81**, 6692 (1997); C. W. Nan, X. Li, and R. Birringer, *J. Am. Ceram. Soc.* **83**, 848 (2000).

¹²C. W. Nan and R. Birringer, *Phys. Rev. B* **57**, 8264 (1998).

¹³T. Y. Chen, G. Wen, and W. C. Liu, *J. Appl. Phys.* **97**, 104312 (2005).

¹⁴B. T. Kelly, *Physics of Graphite* (Applied Science, London, 1981), p. 227.

¹⁵C. N. Hooker, A. R. Ubbelohde, and D. A. Young, *Proc. R. Soc. London, Ser. A* **284**, 17 (1965).

¹⁶J. W. Che, T. Çagin, and W. A. Goddard III, *Nanotechnology* **11**, 65 (2000).

¹⁷G. W. Milton, *The Theory Of Composites* (Cambridge University Press, New York, 2002).

¹⁸Q.-S. Zheng and D. X. Du, *J. Mech. Phys. Solids* **49**, 2765 (2001).

¹⁹D.-X. Du and Q.-S. Zheng, *Acta Mech.* **157**, 61 (2002).